Research Article | Vol. 24, No. 21 | 17 Oct 2016 | OPTICS EXPRESS 23798

Optics EXPRESS

Wide-angle nonmechanical beam steering using liquid lenses

MO ZOHRABI,[1,*] ROBERT H. CORMACK,[1] AND JULIET T. GOPINATH[1,2]

[1] *Department of Electrical, Computer, and Energy Engineering, University of Colorado, Boulder, Colorado, 80309, USA*

[2] *Department of Physics, University of Colorado, Boulder, Colorado, 80309, USA*

[*] *Mo.Zohrabi@colorado.edu*

Abstract: Nonmechanical beam steering is a rapidly growing branch of adaptive optics with applications such as light detection and ranging, imaging, optical communications, and atomic physics. Here, we present an innovative technique for one- and two-dimensional beam steering using multiple tunable liquid lenses. We use an approach in which one lens controls the spot divergence, and one to two decentered lenses act as prisms and steer the beam. Continuous 1D beam steering was demonstrated, achieving steering angles of ±39° using two tunable liquid lenses. The beam scanning angle was further enhanced to ±75° using a fisheye lens. By adding a third tunable liquid lens, we achieved 2D beam steering of ±75°. In this approach, the divergence of the scanning beam is controlled at all steering angles.

OCIS codes: (230.0230) Optical devices; (010.1080) Active or adaptive optics; (280.3400) Laser range finder; (280.3640) Lidar.

References and links

1. Hakki H. Refai, James J. Sluss, and Monte P. Tull, "Digital micromirror device for optical scanning applications," Opt. Eng. **46**, 085401 (2007).
2. C. G. Bachman, *Laser Radar Systems and Techniques* (Artech House, 1979).
3. R. R. Gattass and E. Mazur, "Femtosecond laser micromachining in transparent materials," Nat. Photon. **2**, 219–225 (2008).
4. P. F. Van Kessel, L. J. Hornbeck, R. E. Meier, and M. R. Douglass, "A MEMS-based projection display," Proceedings of the IEEE **86**, 1687–1704 (1998).
5. E. Betzig, and J. K. Trautman, "Near-field optics: microscopy, spectroscopy, and surface modification beyond the diffraction limit," Science **257**, 189–195 (1992).
6. K. C. Neuman and S. M. Block, "Optical trapping," Rev. Sci. Instrum. **75**, 2787–2809 (2004).
7. P. M. Delaney, M. R. Harris, and R. G. King "Fiber-optic laser scanning confocal microscope suitable for fluorescence imaging," Appl. Opt. **33**, 573–577 (1994).
8. T. Ota, H. Fukuyama, Y. Ishihara, H. Tanaka, and T. Takamatsu, "In situ fluorescence imaging of organs through compact scanning head for confocal laser microscopy," J. Biomed. Opt. **10**, 024010 (2005).
9. J. D. Lechleiter, D.-T. Lin, and I. Sieneart "Multi-photon laser scanning microscopy using an acoustic optical deflector," Biophys. J. **83**, 2292–2299 (2002).
10. A. Wehr and U. Lohr, "Airborne laser scanning – an introduction and overview," ISPRS J. Photogramm. Remote Sens. **54**, 68–82 (1999).
11. A. Petrovskaya and S. Thrun, "Model based vehicle detection and tracking for autonomous urban driving," Autonomous Robots **26**, 123–139 (2009).
12. B. D. Duncan, J. B. Philip, and S. Vassili, "Wide-angle achromatic prism beam steering for infrared countermeasure applications," Opt. Eng. **42**, 1038–1047 (2003).
13. B. S. Kim, S. Gibson, and Tsu-Chin Tsao, "Adaptive control of a tilt mirror for laser beam steering," American Control Conference, Proceedings of the 2004. **4**, 3417–3421 (2004).
14. K. Koh, T. Kobayashi, and C. Lee, "A 2-D MEMS scanning mirror based on dynamic mixed mode excitation of a piezoelectric PZT thin film S-shaped actuator," Opt. Express **19**, 13812–13824 (2011).
15. M. G. da Silva, D. W. DeRoo, M. J. Tracy, A. Rybaltowski, C. G. Caflisch, and R. M. Potenza, "Ladar using mems scanning" US Patent 20120236379 A1 (2012).
16. U. Hofmann, J. Janes, and H. -J. Quenzer, "High-Q MEMS Resonators for Laser Beam Scanning Displays," Micromachines **3**, 509 (2012).
17. P. De Dobbelaere, K. Falta, S. Gloeckner, and S. Patra, "Digital MEMS for optical switching," IEEE Communications Magazine **40**, 88–95 (2002).

#273260 http://dx.doi.org/10.1364/OE.24.023798
Journal © 2016 Received 9 Aug 2016; revised 14 Sep 2016; accepted 15 Sep 2016; published 4 Oct 2016
Corrected: 16 November 2016

Optics EXPRESS

18. M. Blum, M. Büeler, C. Grätzel, and M. Aschwanden, "Compact optical design solutions using focus tunable lenses," Proc. SPIE Optical Design and Engineering IV, **8167** 81670 (2012).
19. S. R. Davis, G. Farca, S. D. Rommel, A. W. Martin, and M. H. Anderson, "Analog, Non-Mechanical Beam-Steerer with 80 Degree Field of Regard," Proc. SPIE **6971**, 69710G (2008).
20. D. P. Resler, D. S. Hobbs, R. C. Sharp, L. J. Friedman, and T. A. Dorschner, "High-efficiency liquid-crystal optical phased-array beam steering," Opt. Lett. **21**, 689–691 (1996).
21. Jihwan Kim, Chulwoo Oh, Michael J. Escuti, Lance Hosting, and Steve Serati, "Wide-angle nonmechanical beam steering using thin liquid crystal polarization gratings," Proc. SPIE **7093**, Advanced Wavefront Control: Methods, Devices, and Applications VI, 709302 (2008).
22. J. Lindle, A. Watnik, and V. Cassella, "Efficient multibeam large-angle nonmechanical laser beam steering from computer-generated holograms rendered on a liquid crystal spatial light modulator," Appl. Opt. **55**, 4336–4341 (2016).
23. N. Mukohzaka, N. Yoshida, H. Toyoda, Y. Kobayashi, and T. Hara, "Diffraction efficiency analysis of a parallel-aligned nematic-liquid-crystal spatial light modulator," Appl. Opt. **33**, 2804–2811 (1994).
24. E. Ronzitti, M. Guillon, V. de Sars, and V. Emiliani, "LCoS nematic SLM characterization and modeling for diffraction efficiency optimization, zero and ghost orders suppression," Opt. Express **20**, 17843–17855 (2012).
25. G. Lippmann, "Relations entre les phénomènes électriques et capillaires," Ann. Chim. Phys. **5**, 494 (1875).
26. S. Shian, R. M. Diebold, and D. R. Clarke, "Tunable lenses using transparent dielectric elastomer actuators," Opt. Express **21**, 8669–8676 (2013).
27. M. Blum, M. Büeler, C. Grätzel, and M. Aschwanden, "Compact optical design solutions using focus tunable lenses," Proc. SPIE**8167**, 81670W (2011).
28. N. R. Smith, D. C. Abeysinghe, J. W. Haus, and J. Heikenfeld, "Agile wide-angle beam steering with electrowetting microprisms," Opt. Express **14**, 6557–6563 (2006).
29. S. Terrab, A. M. Watson, C. Roath, J. T. Gopinath, and V. M. Bright,"Adaptive electrowetting lens-prism element," Opt. Express **23**, 25838–25845 (2015).
30. D. Kopp, L. Lehmann, and H. Zappe, "Optofluidic laser scanner based on a rotating liquid prism," Appl. Opt. **55**, 2136–2142 (2016).
31. C. Liu, L. Li, and Q.-H. Wang, "Liquid prism for beam tracking and steering," Opt. Eng. **51**, 114002 (2012).
32. J. Cheng and C.-L. Chen, "Adaptive beam tracking and steering via electrowetting-controlled liquid prism," Appl. Phys. Lett. **99**, 191108 (2011).
33. C. E. Clement and S.-Y. Park, "High-performance beam steering using electrowetting-driven liquid prism fabricated by a simple dip-coating method," Applied Physics Letters **108**, 191601 (2016).
34. B. Berge, "Electrocapillarite et mouillage de films isolants par l'eau," C. R. Acad. Sci.II **317**, 157 (1993).
35. B. Berge and J. Peseux, "Variable focal lens controlled by an external voltage: An application of electrowetting," The European Physical Journal E **3**, 159–163 (2000).
36. H. Ren, and S.-T. Wu, *Introduction to Adaptive Lenses,* (John Wiley and Sons, Inc. 2012).
37. C. U. Murade, J. M. Oh, D. van den Ende, and F. Mugele, "Electrowetting driven optical switch and tunable aperture," Opt. Express **19**, 15525–15531 (2011).
38. R. D. Montoya, K. Underwood, S. Terrab, A. M. Watson, V. M. Bright, and J. T. Gopinath, "Large extinction ratio optical electrowetting shutter," Opt. Express **24**, 9660–9666 (2016).
39. P. Müller, R. Feuerstein, and H. Zappe, "Integrated optofluidic iris," Journal ofMicroelectromechanical Systems **21**, 1156 (2012).
40. C. U. Murade, D. van der Ende, and F. Mugele, "High speed adaptive liquid microlens array," Optics Express **20** 18180–18187 (2012).
41. S. Lee and C. Yang, "Numerical simulation for meniscus shape and optical performance of a MEMS-based liquid micro-lens," Opt. Express **16**, 19995–20007 (2008).
42. K. Mishra, D. van den Ende, and F. Mugele, "Recent Developments in Optofluidic Lens Technology," Micromachines **7**, 102 (2016).
43. J. T. Gopinath, V. M. Bright, C. C. Cogswell, R. D. Niederriter, A. Watson, R. Zahreddine, and R. H. Cormack, "Simulation of electrowetting lens and prism arrays for wavefront compensation," Appl. Opt. **51**, 6618–6623 (2012).
44. Edward A. Watson, "Analysis of beam steering with decentered microlens arrays," Opt. Eng. **32**(11), 2665–2670 (1993).
45. C. Weitkamp, *Lidar: Range-Resolved Optical Remote Sensing of the Atmosphere* (Springer-Verlag, 2005).

1. Introduction

Optical beam scanning methods have a wide range of applications including optical communications [1], light detection and ranging (LIDAR/LADAR) [2], laser micromachining [3], displays [4], microscopy [5], atomic and biophysics [6]. Beam steering is important for fluorescence imaging through confocal [7, 8] and multi-photon microscopy [9]. In atomic physics, optical trapping [6] studies rely on beam control to manipulate the optical trap position and

Optics EXPRESS

Table 1. Summary of beam steering techniques. 1D: one dimensional scan; 2D: two dimensional scan.

Techniques	Steering Method	1D/2D	Maximum steering angle(°)
Scanning mirrors [10]	mechanical	1D/2D	±7 and larger
Rotating prisms [11]	mechanical	1D/2D	45
Piezo actuator [14]	mechanical	1D/2D	15
MEMS mirrors [16]	mechanical	1D/2D	86
Liquid crystal [21, 22]	nonmechanical	1D/2D	±40
Liquid prism [28, 30, 31]	nonmechanical	1D/2D	±26
Liquid lenses (current study)	nonmechanical	1D/2D	±75

stiffness through laser beam angle. Another application, LIDAR, requires wide angle scans to be effective for a variety of applications ranging from mapping to self-driving cars [2, 10, 11].

Beam steering techniques fall into two main categories: mechanical and nonmechanical. Mechanical methods include scanning mirrors [10], rotating prisms [12], piezo actuators [13, 14], and microelectromechanical systems (MEMS) mirrors [15, 16]. Nonmechanical options include acousto-optic deflectors [19], electro-optic deflectors, and liquid crystal spatial light modulator (SLM) [20–22]. While effective, each of these techniques has it's own limitations. For instance, SLMs rely on diffraction; hence the beam steering achieved is not continuous. A typical SLM has a diffraction efficiency of 30–44% [23, 24] resulting in large losses. However, liquid-based, adaptive optical components offer a compact solution. Unfortunately, mechanical parts have a limited lifetime and a better alternative is offered by nonmechanical solutions. For instance, a typical MEMS scanning mirror has a lifetime of 1 million switch cycles [17]. The mean lifetime for nonmechanical devices is significantly longer. In contrast to the MEMS mirror, the tunable lens used in this work has a lifetime that is 40 times longer [18].

There are two types of liquid-based components. The first relies on the electrowetting principle [25], and the other uses a pressure-driven elastic membrane [26, 27]. These devices, which include tunable lenses and prisms, are attractive due to their large range of tunable focal lengths and steering angles, fast response times (ms to s depending on their sizes), low power consumption, and most importantly their robustness, as they have no moving components. Recently, liquid-based prisms have been used to demonstrate 1D and 2D beam steering [28–33]. These studies have used single [28–30] and multiple-liquid [31–33] configurations. However, the steering angles from these compact components are limited; from prisms, the maximum steering reported is ±26° [31]. A brief summary of different beam steering techniques is shown in Table 1. The design we present here has nearly double the maximum beam steering angle of liquid crystals, and nearly triple that of liquid prisms.

In this study, we present a novel method to achieve 1D and 2D beam steering that relies on liquid-based lenses rather than prisms. While prisms can be a straightforward method to achieve beam steering, the use of liquid lenses enables the use of components that are significantly easier to fabricate. Electrowetting-based prisms require multiple electrodes, and pressure-driven prisms, to the best of our knowledge, do not exist. Liquid lenses are commercially available, which makes them an excellent candidate for next-generation, nonmechanical beam steering. These lenses have been studied extensively in other applications [34–36], including implementation as optical switches [37, 38], variable apertures [39], and high speed microlens arrays [40].

Here, we report an optical design based on liquid lenses to demonstrate ultra-wide angle 1D and 2D beam steering while controlling the divergence of the steered beam. We used pressure-driven liquid lenses due to their large aperture, since electrowetting components are limited in size and by gravitational effects. Electrowetting lenses are governed by surface tension and effects of gravity are generally negligible for mm-size optics [41–43]. Specific size limits will

Optics EXPRESS

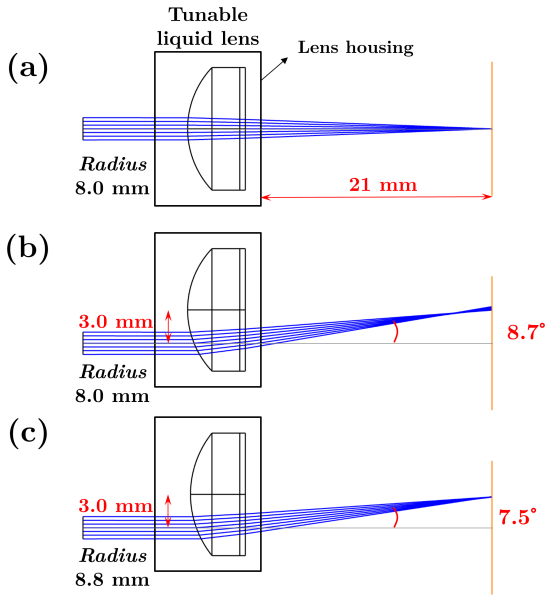

Fig. 1. Steering a beam with a variable focal length lens. (a) A 2 mm collimated beam is focused to an image plane using a centered lens with radius of curvature 8.0 mm. (b) A lens is decentered by 3.0 mm from the optical axis, resulting in steering and defocusing of the beam using 8 mm radius of curvature. The steering angle is 8.7°. (c) The curvature of a variable focal length lens is adjusted to 8.8 mm to minimize the spot size, which results in a shift of the steering angle from 8.7° to 7.5°.

be determined by the density mismatch of the two liquids used in the devices. By utilizing two tunable liquid lenses, we are able to perform continuous one-dimensional beam steering to ±39°, which is further enhanced with a fisheye lens to ±75°. Adding a third liquid lens allows us to accomplish continuous, two-dimensional beam scanning with a cone angle of ±75°.

2. Beam steering principle using liquid lenses

Beam steering has been demonstrated using decentered microlens arrays [44]. We have adopted this approach, combining it with electrically tunable liquid lenses to design a beam steering system. A schematic explaining this concept is depicted in Fig. 1, in which a beam is steered by using a decentered lens. To give an example of the technique, in the figure, a 2-mm collimated beam is focused to a minimum spot size using a single lens (Optotune EL-10-30 [18] with radius of curvature 8.0 mm), as shown in Fig. 1(a). Figure 1(b) shows a configuration in which the lens is shifted by 3.0 mm from the optical axis. This results in a beam steering of 8.7° and a defocusing of the beam. The minimum beam spot size is recovered by changing the curvature of the lens from 8.0 mm to 8.8 mm as shown in Fig, 1(c). As a result, the steering angle changes to 7.5°. The scan can be generated by both positive and negative powers of the off-axis lens. However, modifying the curvature (power) of the scanning lens results in altering the angle of the steered beam. The power change of the scanning lens can be nullified by the addition of a second on-axis lens, positioned before the scan lens as shown in Fig. 2.

By adjusting the curvature of the first lens, we can minimize the spot size while keeping the steering angle fixed. Fig. 2(a) shows an example configuration with lenses with radii of 37 mm and 18.0 mm, respectively. This results in a steering angle of 4.5° with a minimum spot size below the diffraction limit. Changing the radii of the two lenses to 14 mm and 38 mm, respectively, results in a steering angle of 1.2°, as shown in Fig. 2(b). The second lens controls the

Optics EXPRESS

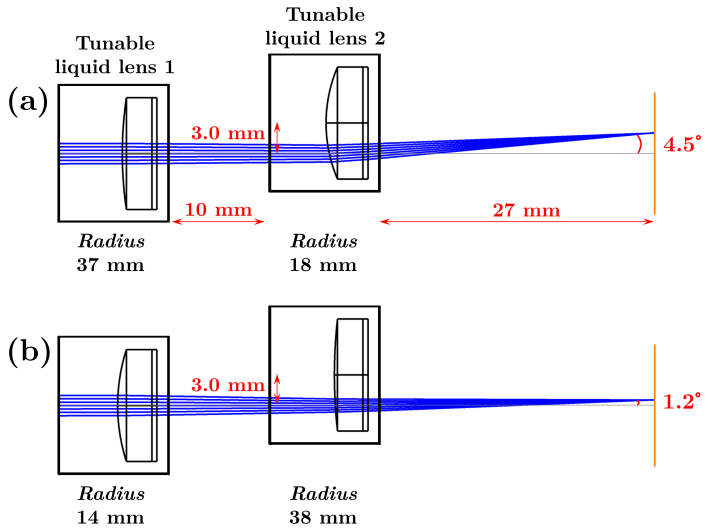

Fig. 2. Schematic examples of adding a second tunable liquid lens used on-axis to compensate for the focal change, resulting in scanning a focused spot over a surface. (a) By adjusting the curvature of the first lens, the spot size is minimized while keeping the steering angle fixed at 4.5°. The radii of the lenses are 37 mm and 18.0 mm, respectively. (b) The curvature of the 2nd lens is changed from 18 mm to 38 mm resulting in steering the beam to 1.2°, while changing the curvature of the 1st lens will minimize the spot size on the image plane.

steering angle of the beam and behaves like a prism. To attain a larger steering angle for a given input beam size, one needs a tunable lens with larger optical power. We have used commercial tunable liquid lenses (Optotune EL-10-30 [18]) with a radius range of 14 to 38 mm (focal length of 50-120 mm). For a 2-mm collimated beam, the optical power range of this lens limits the steering angle change to 5°. This constraint can be improved to ±5° by using an off-axis tunable lens with both positive and negative optical powers, while keeping the aperture size fixed.

To achieve wide angle beam steering, we need to produce a high numerical aperture (NA) source from low NA scanned beam. The solution is to use a relay lens and a diffuser, as shown in Fig. 3(a). A fixed lens is used to image the minimum spot size created by the two tunable lenses onto the diffuser as illustrated in Fig. 3(b). By tuning the liquid lens, we can scan a focused spot over the surface of the diffuser, which then behaves as a point source with a diffusion cone angle of 15°. The diffuser essentially converts the original beam to a high NA light cone, and its location can be controlled by the liquid lens curvature. The physical characteristics of the diffuser surface place a limit on the minimum spot size that can be projected on the diffuser before intensity variations appear in the output cone. This limit for standard glass diffusers made with very fine grit is ~20 m. Using a different approach, one can magnify the scan angle using a backward telescope, however, the beam size will be reduced by the telescope magnification ratio. For instance, for a scan angle of 10–20x, a 1-mm beam diameter reduces to 50–100 m. Such a small beam might be useful for some applications, however, it expands rapidly due to the diffraction. A beam with those characteristics is not useful for LIDAR applications where a more collimated beam is essential. Hence, a combination of a relay lens and a diffuser is a far superior solution.

The high NA beam after the diffuser is used to perform a wide-angle scan with a large size beam (~8–10 mm). We used a pair of lenses after the diffuser to magnify the scan (acting as a wide angle lens with low f-number) and generated a collimated beam at the far field. The

Optics EXPRESS

schematic of the 1D scan setup, including the diffuser and objective lenses, is depicted in Fig. 4. The steering angle of the outgoing beam and the beam size are properties of the lenses used after the diffuser. The setup with the parameters listed in Fig. 4 allows wide-angle beam steering of ±39° (78°).

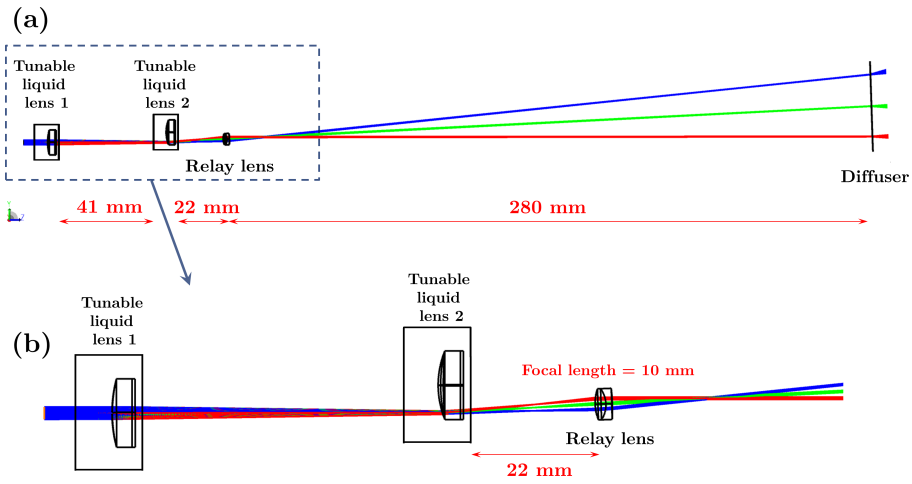

Fig. 3. (a) Schematic of 1D scan using two tunable liquid lenses in conjunction with a relay lens and diffuser simulated in Zemax. The colors represent three different radii of curvature on the second tunable liquid lens. The relay lens images the minimum spot size created by the two tunable lenses onto the diffuser as illustrated in zoomed in view (b). The diffuser behaves as a point source with a diffusion cone angle of 15°. The distances used in the experiment are labeled in the figure.

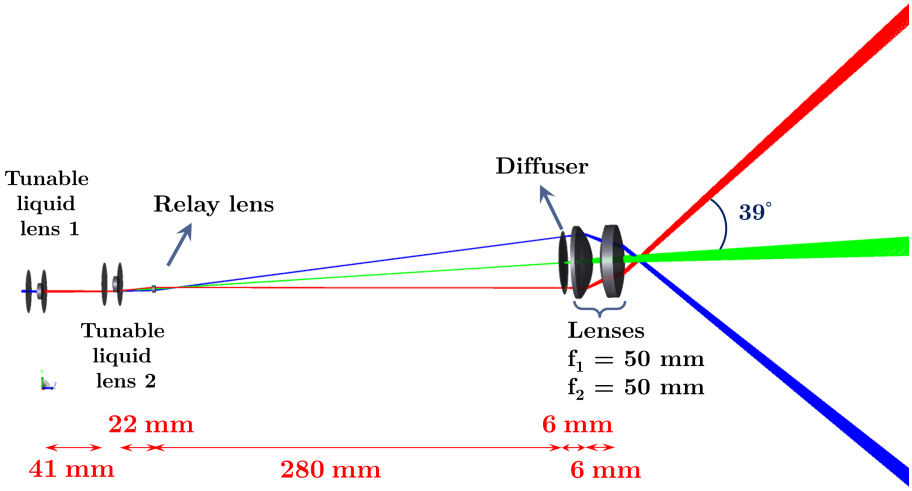

Fig. 4. The schematic of the full 1D scan setup using two tunable liquid lenses. A relay lens is used to position a focused beam on the diffuser. The diffuser acts as a point source with a diffusion cone angle of 15°. The resulting high NA beam is magnified through two lenses. We have used plano-convex and double-convex lenses with a focal length of 50 mm. This configuration results in a beam scanning angle of ±39° with respect to the optical axis of the lenses.

Optics EXPRESS

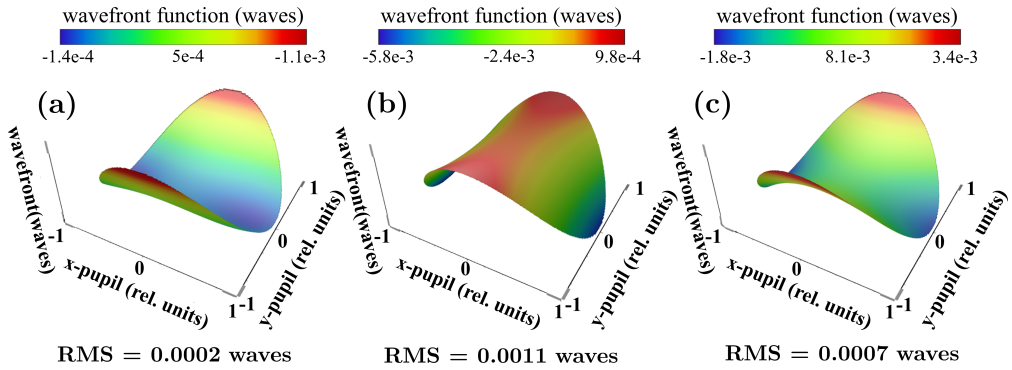

Fig. 5. Modeled wavefront aberrations after the two liquid lens scanner (before the relay lens). (a) Wavefront aberrations for -2.5° with RMS wavefront error of 0.0002 waves. (b) Wavefront aberrations for 0° with RMS wavefront error of 0.0011 waves. (c) Wavefront aberrations for 2.5° with RMS wavefront error of 0.0007 waves. The wavefront error is much smaller than 0.1 waves for all steering angles, and the error is primarily due to spherical aberrations and astigmatism.

We modeled the wavefront aberrations in Zemax after the two tunable liquid lenses using a Gaussian beam. The results are shown in Fig 5. The maximum wavefront error is much smaller than 0.1 waves for all steering angles. The main cause is astigmatism and spherical aberration. This is expected because the two liquid lenses used have a positive optical power and cannot correct spherical aberration and one lens is used off-axis, contributing to astigmatism. Nonetheless, the beam quality is diffraction-limited after our two tunable lens scanner. The wavefront aberrations of the output beam of 1D beam steering after two objective lenses (plano-convex and double-convex lenses with a focal length of 50 mm) are also modeled in Zemax. The final beam quality is far from diffraction-limited – ranging from 1 to 5 waves of wavefront distortion. Here, it is important to note that this is entirely due to the two objective lenses, which are low-cost attempt at essentially a wide-angle camera lens made with two stock singlets (see Fig. 3 and Fig. 4). Again, the primary culprits are spherical aberration and astigmatism. The problem can be easily mitigated with the use of commercial wide-angle lenses, constructed with 9-16 custom elements, that can easily provide diffraction-limited performance. We have used a commercial wide-angle lens for beam scanning, and the results are discussed in section 3.

The steering approach can be extended to 2D scanning with a three-lens system, as shown in Fig. 6. The third tunable lens is decentered perpendicularly to the second tunable liquid lens. By altering the curvature of tunable liquid lenses 2 & 3 (see Fig. 6), we can perform a 2D beam steering. The first tunable liquid lens adjusts the divergence of the scanning spot on the diffuser, while the second tunable liquid lens steers the beam in position on the diffuser. The 2D beam scanning is enhanced by introducing a wide angle fisheye lens to replace the pair of lenses after the diffuser. This results in a 2D hemisphere scan which is modeled in Zemax using a sample fisheye lens from the Zebase library (F_004), as shown in Fig. 7. The simulation shown in Fig 7, predicts a 2D hemisphere scan angle of ±90° (180°).

To summarize, we have implemented a variable lens system to steer the beam. Adding a diffuser to the design is important, as it converts the low numerical aperture beam from the adaptive optical elements to a high numerical aperture cone of light. Lastly, we have used a wide angle lens to convert the high numerical aperture scanned source to a high numerical aperture scanned beam with a controllable divergence.

Optics EXPRESS

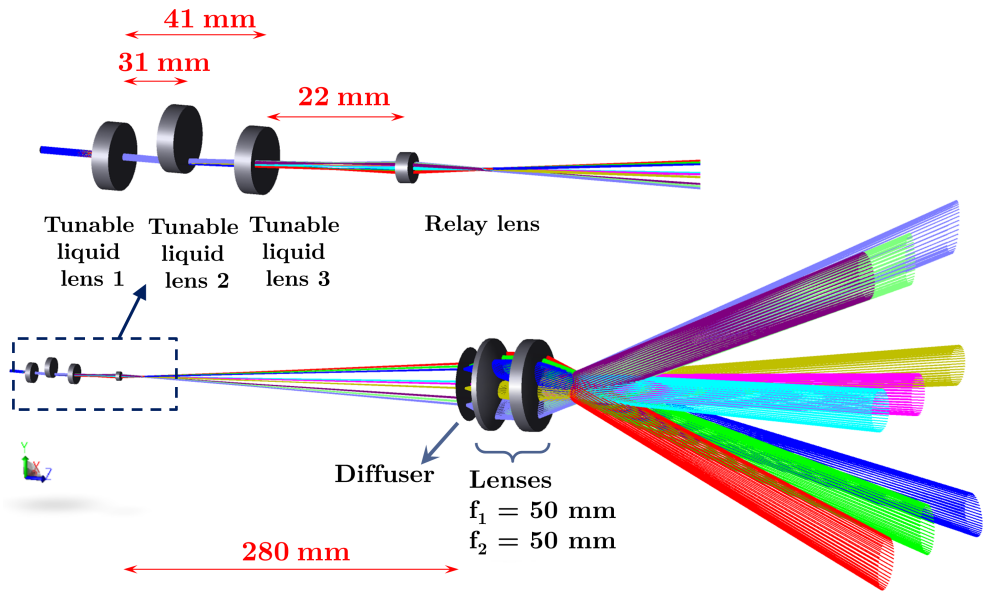

Fig. 6. The schematic of the full 2D scan setup. Adding a third tunable lens perpendicular to the other lenses allows 2D scanning the beam. This configuration results in 2D beam scanning angle of ±39°(78°) in all directions.

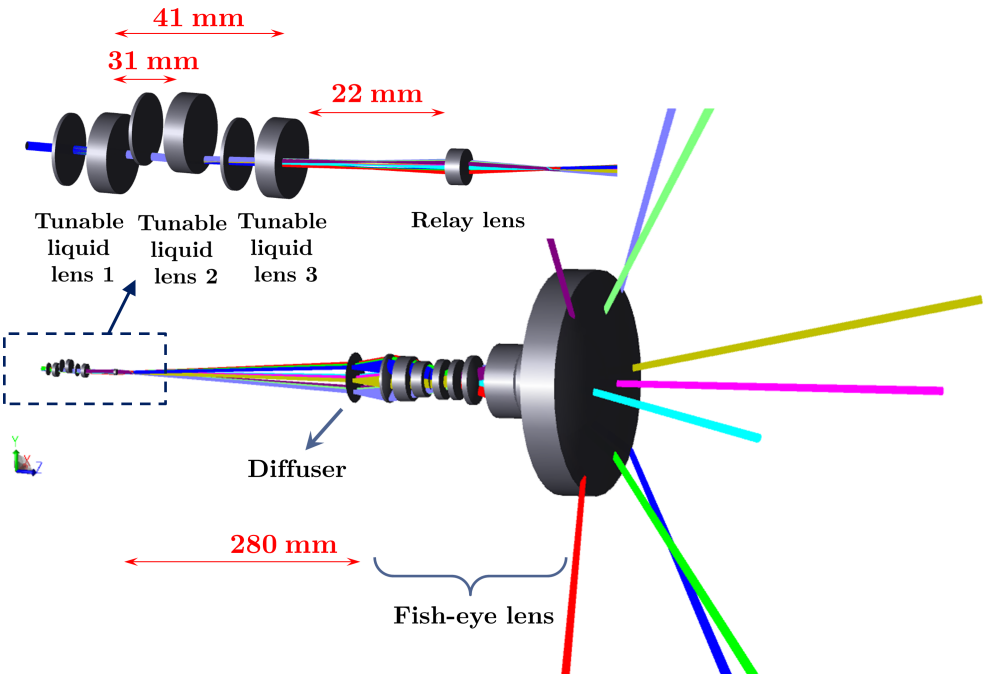

Fig. 7. The schematic of the 2D hemisphere scan using a wide-angle fisheye lens. The fisheye lens replaced the two lenses after the diffuser as shown in Fig. 6. The 2D hemisphere scan is modeled in Zemax using a sample fisheye lens adopted from Zebase library (F_004). This configuration results in 2D beam scanning angle of ±90° (180°) in all directions

Optics EXPRESS

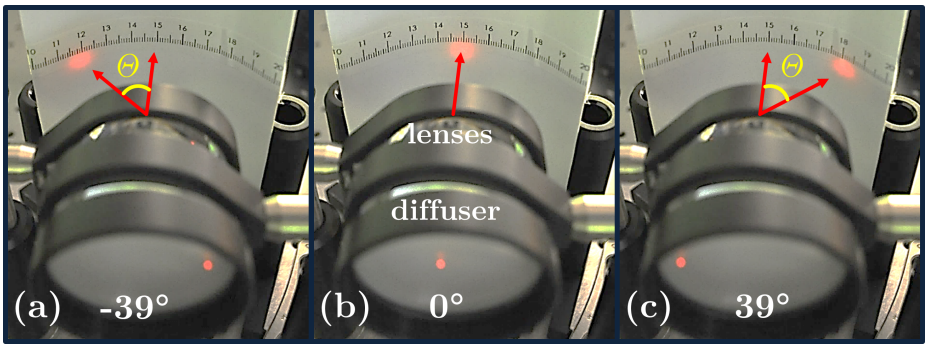

Fig. 8. An example of 1D beam scanning at different steering angles of (a) –39°, (b) 0°, and (c) 39°. The distance between the last objective lens and the imaging setup was kept fixed at 40 mm.

3. Experimental setup and results

3.1. 1D beam scanning using objective lenses

We have demonstrated 1D beam steering experimentally. Figure 4 shows a schematic of our experimental apparatus. A 650 nm cw laser diode was spatially filtered and collimated to 0.6 mm radius. We used two commercially available tunable pressure-driven liquid lenses (Optotune EL-10-30 [18] – with a radius range of 14–38 mm and 10 mm aperture). The first tunable lens was aligned on the optical axis, with the second lens shifted in the plane of the optics table by 4.3 mm. An achromatic doublet lens (focal length of 10 mm), called a relay, lens was positioned after the two tunable lenses to image the minimum spot onto the diffuser [see Fig. 3(b)]. A ground glass diffuser, with diffusion angle of 15°, was placed 28 cm from the relay lens.

After modeling the setup in Zemax, we decided to use a combination of plano-convex and double-convex lenses after the diffuser (both have a focal length of 50 mm). By changing the curvature of the first liquid lens, we are able to adjust the beam divergence. Altering the curvature of the second liquid lens results in steering the beam. The outgoing beam is then imaged onto a camera (Chameleon CMLN-13S2M-CS) using a lens. The imaging setup was placed 40 mm from the last lens as shown in Fig. 8(a)–8(c). An example of beam steering using two objective lenses is photographed in Fig. 8(a)–8(c).

The steering angle, θ, is evaluated from the lateral displacement of the beam with respect to the optical axis of the setup [see Fig. 8(a)–8(c)]. For a specified steering angle, multiple images were acquired by changing the curvature of the first lens. Every image was fitted to a Gaussian function and its area was evaluated from the beam waist ($1/e^2$ Gaussian function) along the horizontal and vertical directions. The offset of the second tunable lens was optimized experimentally, and we were able to generate a large scan from –39° to 39° (78° total) as shown in Fig. 8(a)–8(c). This result is in agreement with the Zemax model presented in the previous section. The result of a full scan at different steering angles is plotted in Fig. 9. The density plot color represents the area of the scanning beam imaged onto the camera (spot size) as a function of diopters of the first tunable lens and steering angle controlled by the second tunable lens. The area of the scanning beam varies between 0.2–0.7 mm^2. It is clear from the figure that the beam divergence can be simply adjusted by the first tunable lens at any steering angle. The ability to steer the beam at large angles while being able to adjust the beam divergence is a powerful tool. For example, the ability to control the beam divergence can improve the spatial resolution in applications such as microscopy, optical tracking, and LIDAR systems.

Optics EXPRESS

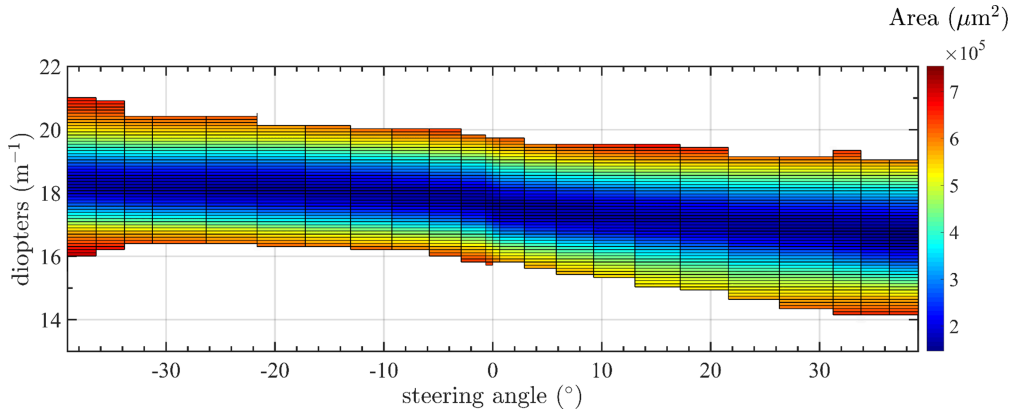

Fig. 9. Density plot representing the area of the outgoing beam as a function of diopters of the first tunable lens and steering angle of the second tunable lens. By using two objective lenses after the diffuser, we were able to steer the beam from –39° to 39° while adjusting the scanning beam divergence using the first liquid lens.

3.2. 1D beam scanning using a fisheye lens

The beam steering technique described earlier was further enhanced by replacing the two objective lenses after the diffuser with a wide angle fisheye lens (Olympus M.Zuiko ED 8 mm f/1.8). By using the fisheye lens, we were able to achieve a beam scan of –75° to 75° (150° total). The limitation in the scan range is due to vignetting at the back aperture of our fisheye lens. Reaching larger scan angles is feasible by matching the cone of light after the diffuser to the entrance pupil of the fisheye lens. This can be resolved by using a larger aperture wide angle lens. An example of the scan is photographed and shown in Fig. 10(a)–10(c). The result of a full scan at various steering angles is plotted in Fig. 11. The colors in the density plot represent the area of the scanning beam as a function of diopters of the first tunable lens and steering angle of the second tunable lens. We were able to scan the beam from –75° to 75° with its area varying between 0.07–0.14 mm^2. The beam size was then adjusted by controlling the curvature of the first tunable lens. This method can produce a wide-angle scanning beam with controllable beam divergence as shown in Fig. 10 and Fig. 11.

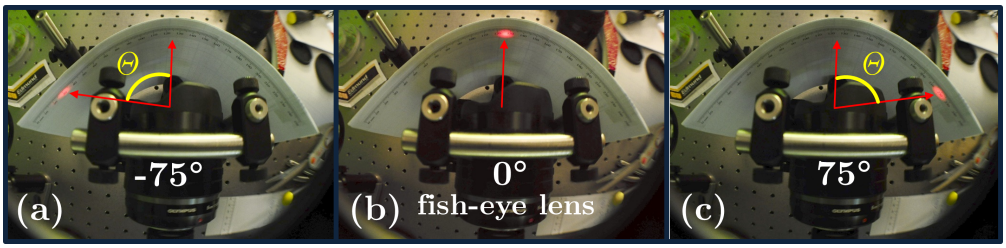

Fig. 10. An example of 2D beam scanning at different steering angles of (a) –75°, (b) 0°, and (c) 75° using a commercial fisheye lens. The distance between the last objective lens and the imaging setup was kept fixed at 40 mm.

3.3. 2D beam scanning using a fisheye lens

We added a third tunable liquid lens to the experiment to perform wide-angle 2D beam scanning. The schematic of the experimental setup is shown in Fig. 6 and Fig. 7. The electrical current

Optics EXPRESS

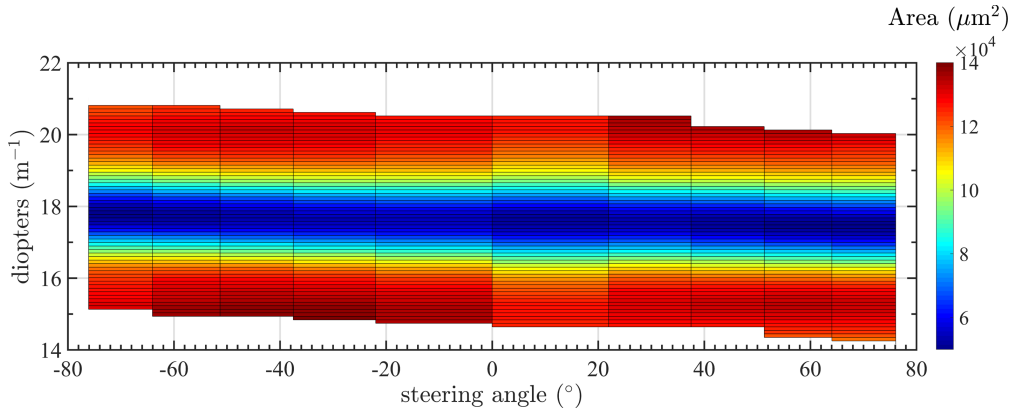

Fig. 11. Density plot representing the area of the outgoing beam as a function of diopters of the first tunable lens and steering angle of the second tunable lens. By using a commercial fisheye lens after the diffuser, we were able to steer the beam from –75° to 75° while adjusting the scanning beam divergence.

through all three lenses were controlled using MATLAB. We changed the curvature of the second and third lenses by adjusting the current and demonstrated 2D beam scanning. To implement the scan, we generated a 2D matrix of the curvatures needed. The focal length measurement for a tunable liquid lens as a function of current is fitted to a linear function. Hence, any arbitrary scanning angle can be achieved by dialing the appropriate curvature values (current values from the fit). Similarly, the curvature of the first tunable lens adjusts the size of beam on the diffuser (altering the divergence of the outgoing beam). We imaged the outgoing beam onto the camera, which was kept fixed at a 40 mm distance from the last lens.

Figure 12 shows an example of images acquired at various steering angles. The beam was scanned horizontally and vertically from –75° to 75°. Figure 12(a) shows the minimum spot size at different steering angles horizontally and vertically. Figure 12(b) displays images of the beam spot at various steering angles after changing the focal length of the first tunable lens by 8 mm. The absolute focal length number is different at every angle in Fig. 12(a), however, the difference in the focal length (8 mm) was kept fixed at all angles to generate Fig. 12(b). The areas of the minimum spot at (0°,0°) and (0°,–75°) are 0.071 mm^2 and 0.068 mm^2, respectively [see Fig. 12(a)], which then become 0.129 mm^2 and 0.112 mm^2 after changing the focal length by 8 mm [see Fig. 12(b)]. This method can be implemented in many airborne and ground-based LIDAR systems, where wide-angle scans are required. Typical beam divergences for LIDAR systems are 0.1–2 mrad, and are often controlled with beam expansion optics [45]. Our system offers an elegant nonmechanical alternative to control the beam divergence. In addition, beam diameters for LIDAR typically range from a few cm to tens of meters, depending on the target size [45]. Our current design has the ability to generate few mm to few cm beam diameter.

4. Conclusion

In conclusion, we have demonstrated one- and two-dimensional beam steering based on tunable liquid lenses. Our novel technique using liquid lenses is modeled in Zemax and experimentally verified. We were able to achieve 1D beam steering ±39° (78°) using two liquid lenses. The results were further enhanced by using a wide-angle fisheye lens to ±75°(150°). Adding a third tunable liquid lens enables us to perform a 2D beam scanning of ±75° in all directions. In addition, we have shown that we were able to control the beam divergence of the outgoing beam by tuning one of the liquid lenses. Our design using liquid lenses can be easily used in the visible

Optics EXPRESS

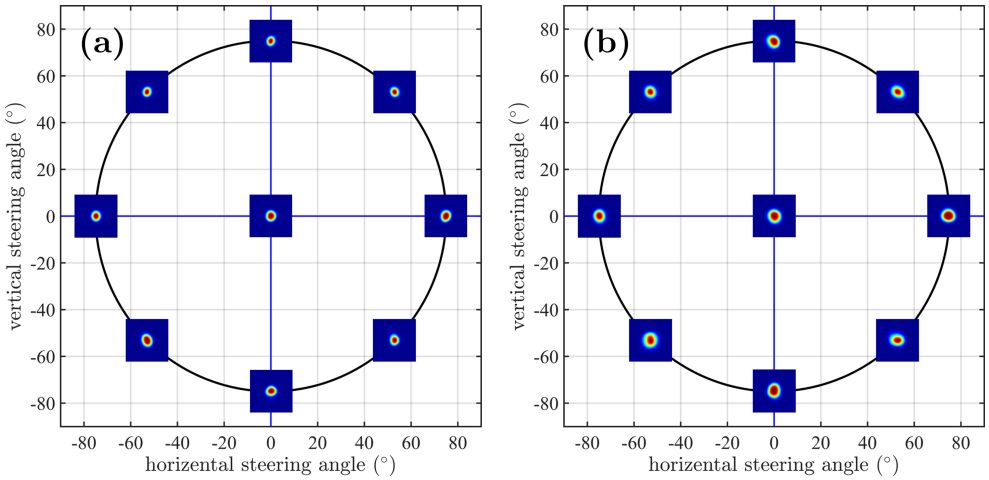

Fig. 12. An example of 2D beam scanning at different steering angles using a commercial fisheye lens. The beam was scanned horizontally and vertically between –75° to 75°. (a) Images of the minimum spot size after adjusting the focal length of the first tunable lens. The images shown here are not represented as actual size for display purposes, but are all on the same scale. (b) Images of the spot on the camera after changing the focal length of the first lens by 8 mm. Note that the spot size is here visibly larger than in (a).

and near-infrared wavelengths regions.

The steering demonstrated here is far superior to any nonmechanical scan demonstrated to date, and it has a potential for LIDAR applications where a large steered beam is crucial. Autonomous driving systems use 2D scanning LIDAR based on mechanical beam steering. However, the fast response time, low power consumption, low cost, and the ability to be miniaturized make our nonmechanical beam steering approach an attractive candidate for these applications. There are a few methods to miniaturize our optical design, such as smaller output optics (*i.e.* fisheye lenses), folded optics to reduce the distance between the relay lens and the diffuser, and multiple liquid lenses to achieve larger beam steering.

Acknowledgments

The authors would like to acknowledge Dr. J. Thayer (Univ. of Colorado Boulder) for helpful discussions.

Funding

Office of Naval Research (ONR) (W0014-14-1-2739); University of Colorado Boulder Libraries Open Access Fund.